

Cite this: *Dalton Trans.*, 2025, **54**, 6313Received 19th February 2025,
Accepted 19th March 2025

DOI: 10.1039/d5dt00416k

rsc.li/dalton

A biologically inspired iron complex for the homogeneous reduction of Cr(VI) to Cr(III)†

Kelly L. Gullett,^a Jewelianna M. Moore,^b Courtney L. Ford^a and Alison R. Fout^{id}*^b

Hexavalent chromium (Cr^{VI}) is a toxic and carcinogenic pollutant commonly found in industrial waste, posing significant environmental and health risks. In contrast, trivalent chromium (Cr^{III}) is significantly less toxic and less mobile in water. This study presents the efficient reduction of Cr^{VI} to Cr^{III} using a biologically inspired non-heme iron complex, [N(afa^{Cy})₃Fe^{II}OTf]OTf. The reaction achieves near-quantitative conversion as calculated by a paramagnetic ¹H NMR calibration method for direct quantification of the iron(III)-oxo species formed during reduction. X-ray photoelectron spectroscopy (XPS) confirms Cr^{III} as the final chromium containing product. This work provides a highly effective and selective approach to chromium detoxification, with potential applications in water remediation while demonstrating the utility of a ¹H NMR calibration curve for quantifying paramagnetic species in reaction mixtures.

Introduction

Chromium occurs naturally in volcanic emissions, rocks, animals, plants, soil, and water.¹ However, improper waste management in industrial processes such as leather tanning, chrome plating, and the manufacturing of industrial dyes and pigments significantly increases chromium levels in ground and drinking water.^{2,3} Chromium primarily exists in two oxidation states: Cr^{VI} and Cr^{III}.⁴ The hexavalent form (Cr^{VI}) is commonly found in water and is carcinogenic to humans when inhaled, posing occupation risk to workers in manufacturing plants.³ While extensive research has focused on inhalation risks of Cr^{VI}, recent studies highlight concerns regarding oral toxicity due to hexavalent chromium's prevalence in water. Its ingestion is highly toxic to plants, animals, and humans,^{3,5} as it can infiltrate cells through the sulfate uptake pathway in plants and lower organisms.⁶ Additionally, Cr^{VI} ingestion increases the risk of gastrointestinal and liver cancer in humans,¹ presenting a serious public and environmental health concern. Hexavalent chromium's high water mobility presents substantial challenges for its removal from drinking water sources.

In contrast, trivalent chromium (Cr^{III}) has 100-fold lower toxicity and is less mobile in water,^{4,7–9} typically forming solid oxides or hydroxides, depending on system pH.^{10,11}

Consequently, significant research has focused on the removal of Cr^{VI}, or its reduction to less toxic Cr^{III}.¹² Recent advancements include electrochemical and photochemical reduction methods,^{11,13} reflecting ongoing efforts to mitigate chromium contamination in water.

Previous work in the Fout Lab utilized a tripodal iron complex, [N(afa^{Cy})₃Fe^{II}OTf]OTf (**1**) (N(afa^{Cy})₃ = tris(5-cycloimino-pyrrol-2-ylmethyl)amine, OTf = triflate) for the reduction of various oxyanions, including nitrogen, chlorine, and selenium-containing oxyanions to: nitric oxide,^{14–16} ammonia,²⁶ or nitrogen;²⁶ chloride;^{16,17} and red elemental selenium¹⁸ respectively. In these reactions, the formation of a terminal iron(III)-oxo ([N(afa^{Cy})₃FeO]OTf) (**2**) is stabilized through hydrogen bonding to the secondary coordination sphere. While these oxyanions have positive reduction potentials, they are generally considered kinetically inert due to their low binding affinity to metal centers.^{16,19} In contrast, Cr^{VI} is a powerful oxidant widely used in organic reactions, such as the oxidation of alcohols to ketones and carboxylic acids.^{20–22} Historically, it has also been employed as an oxidant in inorganic systems.²³ Given the previous success in oxyanion reduction, we aimed to reduce carcinogenic Cr^{VI} compounds to relatively benign Cr^{III} utilizing **1**.

Results and discussion

Initial attempts at chromium oxyanion reduction using K₂CrO₄ showed limited reactivity due to its poor solubility in organic solvents, even after 16 hours at room temperature. The addition of solubilizing agents such as methanol and crown ethers enhanced the formation of **2** but failed to yield reproducible results. Furthermore, protodemetalated (or acidified)

^aSchool of Chemical Science, University of Illinois at Urbana-Champaign, 600 S. Mathews Ave., Urbana, Illinois 61801, USA

^bDepartment of Chemistry, Texas A&M University, 580 Ross St. College Station, Texas 77843, USA. E-mail: fout@tamu.edu

† Electronic supplementary information (ESI) available: For experimental details. See DOI: <https://doi.org/10.1039/d5dt00416k>



ligand formation was observed by ^1H NMR spectroscopy, prompting the addition of triethylamine to the reaction mixture.

To overcome these challenges, we shifted our focus to $[\text{TBA}]_2\text{Cr}_2\text{O}_7$ (TBA = tetrabutylammonium), a more soluble and commercially available hexavalent chromium salt. The addition of one equivalent of $[\text{TBA}]_2\text{Cr}_2\text{O}_7$ to **1** (7 equivalents) in acetonitrile, along with one drop of triethylamine to discourage protodemetalated ligand formation, resulted in an immediate and dramatic colour change from yellow to dark brown (Scheme 1, top). This striking transformation suggested the previous lack of reactivity with K_2CrO_4 was likely due to incompatible solubilities rather than an inability of **1** to deoxygenate the chromium oxyanion.

Analysis of the crude reaction mixture by paramagnetic ^1H NMR spectroscopy after 30 minutes revealed the formation of **2**, trace amounts of unreacted **1**, and a small quantity of the previously published paramagnetic impurity $\text{N}(\text{pi}^{\text{Cy}})_3\text{Fe}$ (**3**),²⁴ by comparison of the ^1H NMR spectra to the isolated complexes. The formation of complex **3** is likely due to the inclusion of triethylamine, and the exclusion of triethylamine in subsequent reactions, prevented the formation of **3**, and showed no evidence of protodemetalated ligand, contrasting the reduction of K_2CrO_4 .

As a small amount of unreacted **1** persisted in dichromate reduction, we sought to quantify the reaction between **1** and dichromate. Previous quantification methods for oxyanion reduction in this system relied on indirect approaches, using external reductants such as 1,2-diphenylhydrazine (DPH) or triphenylphosphine (PPh_3), along with chemical traps such as cobalt tetraphenylporphyrin (CoTPP).^{18,25,26} These methods formed diamagnetic products quantifiable *via* ^1H or ^{31}P NMR spectroscopy, which were not applicable in dichromate reduction. Instead, we turned to direct quantification of **2** *via* paramagnetic ^1H NMR spectroscopy.

While many research groups, including ours, successfully use ^1H NMR spectroscopy to analyse paramagnetic complexes, its application for quantification remains challenging. Although we routinely employ this technique to study our iron complexes, the presence of multiple paramagnetic species

with different oxidation states complicates direct integration against a paramagnetic standard, preventing accurate quantification.^{27,28}

In diamagnetic ^1H NMR spectroscopy, resonances are typically integrated against a known standard for quantitative analysis of reaction yields. However, applying this approach to mixtures of paramagnetic compounds is challenging due to resonance broadening, which results from rapid electron relaxation affecting nuclear relaxation times. These effects depend on both the oxidation state and the identity of the paramagnetic metal center.^{27,28}

Hazari *et al.* successfully quantified a paramagnetic nickel complex by ^1H NMR spectroscopy through integration against a cobaltocene reference. However, their system contained only a single paramagnetic product, simplifying the analysis.²⁹ In contrast, as demonstrated in Fig. 1, direct integration of resonances from high-spin Fe^{II} and high-spin Fe^{III} compounds, such as $[\text{N}(\text{afa}^{\text{Cy}})_3\text{Fe}^{\text{II}}\text{OTf}]\text{OTf}$ (**1**) and $[\text{N}(\text{afa}^{\text{Cy}})_3\text{Fe}^{\text{III}}\text{O}]\text{OTf}$ (**2**) respectively, yields unequal values for comparable peaks in the ^1H NMR spectra. This discrepancy arises from oxidation state dependent differences in relaxation times, which unevenly affect the nuclear relaxation of hydrogen atoms in each complex.³⁰

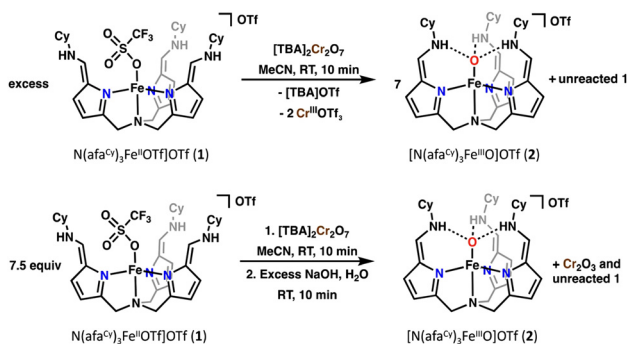
To quantify the yield of **2**, we developed a calibration curve correlating the relative ^1H NMR resonances of **1** and **2** to their solution ratios (Fig. 1, top left). This approach provides a direct and reliable means of calculating the yield during the oxidation of **1** to **2** in the presence of oxyanions (see Experimental section), eliminating the need for additional reactions or external reductants and enabling more straightforward and accurate quantification.

The reduction of $[\text{TBA}]_2\text{Cr}_2\text{O}_7$ was repeated with an excess of **1**, and the resulting ^1H NMR spectra were analysed using the calibration curve (Scheme 1, top). To ensure accuracy, three aliquots were taken from the reaction mixture. The experiment was further replicated with varying excesses of **1** to assess the calibration curve's reliability across different 1:2 ratios (see ESI, Tables S1–S3†).

In the first test, using 24.5 equivalents of **1**, three aliquots were taken after stirring with dichromate at room temperature for 20 minutes, followed by two additional aliquots after 60 minutes. Analysis of the five resulting ^1H NMR spectra indicated a 97.7% yield of **2** after 60 minutes. Repeating the experiment with 32 equivalents of **1** and collecting three aliquots after 10 minutes of stirring yielded a calculated 99.5% conversion, demonstrating near-quantitative formation of **2**.

After quantifying the formation of **2** during dichromate reduction, we sought to determine the oxidation state of the resulting chromium species using X-ray photoelectron spectroscopy (XPS). Dichromate contains two Cr^{VI} centers, and if all electrons generated during the stoichiometric oxidation of **1** are utilized to reduce dichromate, a mixture of Cr^{III} and Cr^{II} products would be expected. However, given the rarity of Cr^{II} formation in chromate or dichromate reduction,^{11,31,32} we hypothesize that the primary product of $[\text{TBA}]_2\text{Cr}_2\text{O}_7$ reduction by **1** is Cr^{III} .

XPS analysis of the stoichiometric crude reaction mixture proved challenging due to the low concentration of Cr relative



Scheme 1 Synthesis of **2** and Cr^{III} products from the reduction of $[\text{TBA}]_2\text{Cr}_2\text{O}_7$.



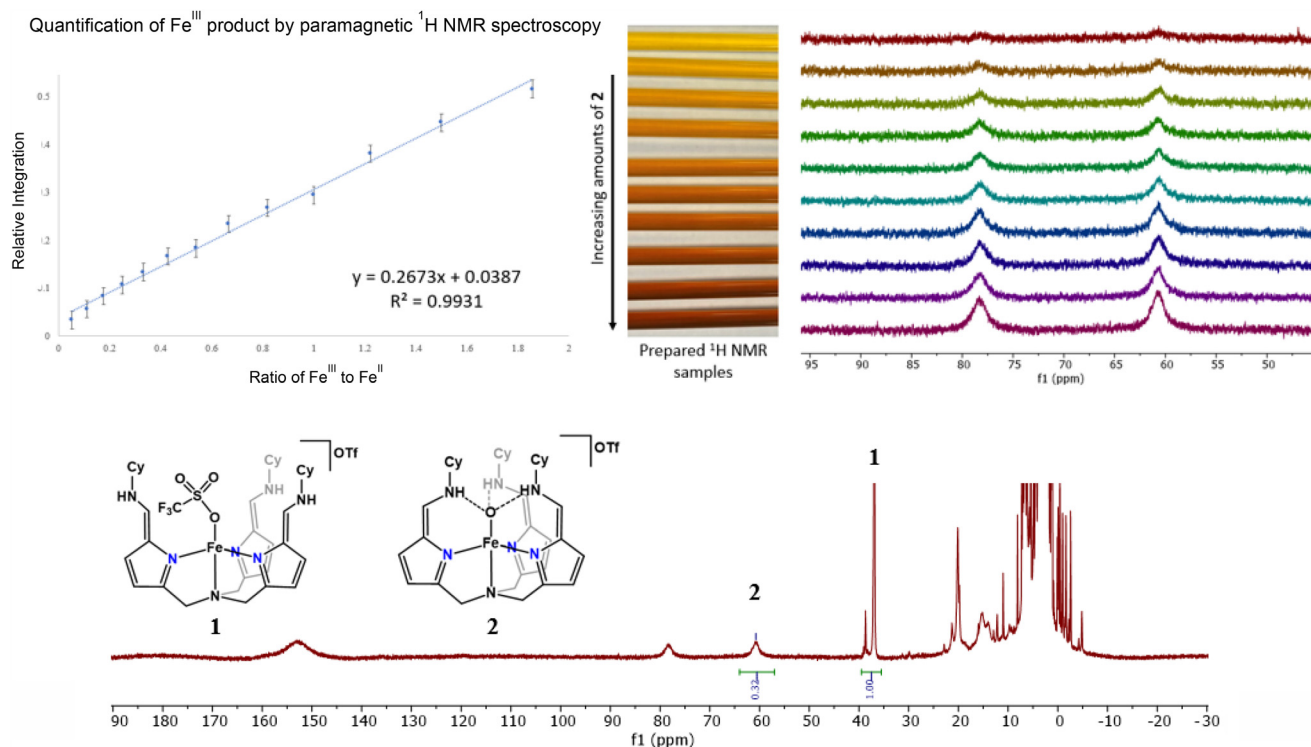


Fig. 1 Quantification of [N(afa^{Cy})₃Fe^{II}(OTf)]OTf (**1**) and [N(afa^{Cy})₃Fe^{III}(O)]OTf (**2**) using ¹H NMR spectroscopy. Calibration curve (top left) is displayed along with samples corresponding to various amounts of **1** and **2** (top right). Representative ¹H NMR spectrum is shown (bottom).

to that of **2**. Attempts to isolate the Cr species through standard work-up procedures including sequential washes with increasingly polar solvents, did not yield noticeable precipitation of Cr products.

We hypothesized that the soluble Cr^{III} cation remained in solution interacting with excess triflate anions, preventing the formation of triflic acid and avoiding protodemetalation of the ligand. Unlike the reduction of K₂CrO₄, which was not quantitative and led to an excess of triflate anions without a proper counter cation, reactions with [TBA]₂Cr₂O₇ resulted in the excess triflate anions interacting with the Cr^{III} cation, maintaining solubility.

To generate an insoluble Cr product, an aqueous sodium hydroxide (NaOH) solution was added to the reaction mixture (Scheme 1, bottom), resulting in the formation of a red-brown precipitate. The solid was isolated, dried, and analyzed *via* XPS,^{10,13} which confirmed its identity as Cr^{III} oxide.^{33,34}

Experimental

General considerations

All manipulations were carried out in the absence of water and dioxygen, due to the air and moisture sensitivity of the compounds, using a Vigor or mBraun inert atmosphere glovebox under an argon atmosphere unless otherwise specified. All glassware was dried in an oven for at least 4 h and cooled in an evacuated antechamber prior to use. Acetonitrile (MeCN) was

dried and deoxygenated on a Vigor Solvent Purification System and stored over 3 Å molecular sieves, purchased from VWR, prior to use. Methanol (MeOH) It was stirred over calcium hydride then distilled, degassed, and stored over 3 Å molecular sieves, purchased from VWR, prior to use. Deuterated solvents were purchased from Cambridge Isotope Laboratories and stored over 3 Å molecular sieves prior to use. Celite 545 (J. T. Baker) was heated to 150 °C under dynamic vacuum for 24 h prior to use in the glovebox. All reagents were purchased from commercial sources and used as received unless otherwise noted. Bis(tetrabutylammonium) dichromate ([TBA]₂Cr₂O₇) was dissolved in MeCN and stored over 3 Å sieves for 72 hours in a taped vial, filtered and recrystallized prior to use. [TBA]₂Cr₂O₇ was used in the dark, as colour changes were noted upon exposure to light. Potassium chromate was recrystallized from a saturated aqueous solution layered with methanol and cooled to 0 °C. 1,2-Diphenylhydrazine was recrystallized twice with concentrated solutions of diethyl ether with hexanes layering before use and stored at -35 °C. [N(afa^{Cy})₃Fe(OTf)]OTf (**1**)²⁴ and [N(afa^{Cy})₃Fe(O)]OTf (**2**)¹⁴ were synthesized according to literature procedures. X-ray photoelectron spectroscopy was performed at the Materials Characterization Facility at Texas A&M University (Research Resource ID [RRID: SCR_022202]). The data was acquired using OmicronESCA+ with a Mg X-ray source; emission current 20 mA, voltage 15KV and fit using the accompanying software.

NMR measurements. For generation and use of the calibration curve, all ¹H NMR spectra were recorded at ambient



temperature on a Bruker Avance Neo console operating at 500 MHz (^1H NMR) in CD_3CN . ^1H NMR spectra were recorded with a standard zg30 pulse sequence, 32 scans, with an acquisition time of 0.2621 s and relaxation delay of 1.0 s. When processing the spectral data, the apodization was set to 4 Hz, a polynomial fit baseline correction was applied, and the spectra were referenced to residual solvent (MeCN, 1.94 ppm). Line shape analysis to determine linewidth at half height ($\Delta\nu_{1/2}$) was accomplished with MestReNova NMR spectroscopy software.

Generation of calibration curve. 5 mM stock solutions of **1** and **2** were made in MeCN. Known quantities (see Tables S1–S3†) of both solutions were added to a 20 mL scintillation vial, followed by removal of volatiles under reduced pressure. The resulting residue was dissolved in 0.8 mL of CD_3CN and transferred directly to an oven dried NMR tube followed by analysis. This experiment was repeated in triplicate for statistical relevance (Tests 1–3).

Procedures for hexavalent chromium reduction and quantification

Chromate reduction and quantification. A 20 mL scintillation vial was charged with **1** (0.0561 g, 0.0600 mmol), K_2CrO_4 (0.0029 g, 0.0150 mmol), crypt-222 (0.0113 g, 0.0300 mmol), 3 mL acetonitrile, and 1 mL methanol. The solution was stirred 16 h and evacuated to dryness *in vacuo*. The residue was analysed by ^1H NMR spectroscopy, which showed the residue contained **2**, $\text{H}_3\text{N}(\text{pi}^{\text{Cy}})_3\cdot 3\text{HOTf}$, and unreacted **1** (Fig. S2†).

Repeating the reaction in the presence of NET_3 (0.0061 g, 0.0600 mmol) precluded the formation of $\text{H}_3\text{N}(\text{pi}^{\text{Cy}})_3\cdot 3\text{HOTf}$. The amount of **2** furnished from the reaction was determined by triturating the dried crude reaction mixture with diethyl ether, redissolving the residue in 4 mL acetonitrile, adding 1,2-diphenylhydrazine (0.0111 g, 0.0600 mmol), and stirring the solution for 16 h. Volatiles were removed under reduced pressure and the dark red powder obtained was washed with 3 mL diethyl ether and filtered over a pad of Celite to isolate the azobenzene and 1,2-diphenylhydrazine. The diethyl ether wash was dried under vacuum and analysed by ^1H NMR spectroscopy (Fig. S3;† ferrocene was added as an internal standard; 0.0056 g, 0.0300 mmol), revealing a 31% conversion of 1,2-diphenylhydrazine to azobenzene, which is equivalent to the reduction of 2.47 equiv. of **2** (4.00 equiv. expected).¹⁶

Stoichiometric reduction of bis(tetrabutylammonium) dichromate by $[\text{N}(\text{afa}^{\text{Cy}})_3\text{Fe}(\text{OTf})]\text{OTf}$. To a 20 mL scintillation vial was added **1**, (0.035 mmol, 0.0327 g), bis(tetrabutylammonium) dichromate (0.005 mmol, 0.0035 g), 4 mL of MeCN and 1 drop triethylamine. The reaction was allowed to stir for 30 minutes, then half of the solution was transferred to a clean 20 mL scintillation vial, followed by removal of volatiles under reduced pressure. The resulting brown residue was analysed by ^1H NMR spectroscopy (Fig. S4†).

Reduction of bis(tetrabutylammonium) dichromate *via* $[\text{N}(\text{afa}^{\text{Cy}})_3\text{Fe}(\text{OTf})]\text{OTf}$ for quantification of **2.** A 2.5 mM stock solution of bis(tetrabutylammonium) dichromate was made in MeCN. To a 20 mL scintillation vial was added **1** (0.0605 mmol, 0.0566 g) and 5 mL of MeCN. The solution was

allowed to stir for 5 minutes to ensure solubilization of **1**. 1 mL of the bis(tetrabutylammonium) dichromate stock solution (0.0025 mmol) was added to the stirring solution of **1**. The reaction was allowed to stir at room temperature for 20 minutes, followed by removal of three 1 mL aliquots of the reaction solution. The aliquots were transferred to 20 mL scintillation vials, and volatiles were removed under reduced pressure. The resulting residues were dissolved in 0.8 mL of CD_3CN and transferred directly to oven dried NMR tubes followed by analysis *via* ^1H NMR spectroscopy. The remainder of the reaction solution was allowed to stir for an additional 40 minutes. Two additional aliquots were removed from the reaction solution and treated as described above.

A second trial of this reaction was then repeated to ensure accuracy. To a 20 mL scintillation vial was added **1** (0.04 mmol, 0.0374 g) and 3.5 mL of MeCN. The solution was allowed to stir for 5 minutes to ensure solubilization of **1**. 0.5 mL of the dichromate stock solution (0.00125 mmol) was added to the stirring solution of **1**. The reaction was allowed to stir at room temperature for 10 minutes, followed by removal of three 1 mL aliquots of the reaction solution. The aliquots were transferred to 20 mL scintillation vials, followed by removal of volatiles under reduced pressure. The resulting residues were dissolved in 0.8 mL of CD_3CN and transferred directly to oven dried NMR tubes followed by analysis *via* ^1H NMR spectroscopy.

Large scale reduction of bis(tetrabutylammonium) dichromate for collection of chromium containing products. To a 20 mL scintillation vial was added **1**, (0.400 mmol, 0.374 g), bis(tetrabutylammonium) dichromate (0.057 mmol, 0.040 g), and 20 mL of MeCN. The reaction was allowed to stir for 20 minutes, followed by removal of the scintillation vial from the glovebox. NaOH (0.342 mmol, 0.0137 g) was dissolved in 0.4 mL of water and added to the reaction mixture. Immediate precipitation of a red-brown powder was observed. The solution stirred for an additional 10 min followed by collection of the precipitate *via* centrifuge. The precipitate was washed with 20 mL of MeCN, acetone, and dichloromethane (DCM), then transferred to a clean 20 mL scintillation vial. The vial was placed in a vacuum oven at 50 °C for 16 hours to remove residual water. The powder was then analysed by X-ray photoelectron spectroscopy (XPS) which revealed formation of Cr^{III} oxide (see Fig. S6†).

Conclusions

In summary, we have demonstrated the successful reduction of Cr^{VI} to less hazardous Cr^{III} using a biologically inspired non-heme iron complex, $[\text{N}(\text{afa}^{\text{Cy}})_3\text{Fe}^{\text{II}}\text{OTf}]\text{OTf}$ (**1**). The reaction proceeds with near-quantitative efficiency, as confirmed through quantitative paramagnetic ^1H NMR utilizing a novel calibration curve, enabling direct and accurate quantification of the iron(III)-oxo species, $[\text{N}(\text{afa}^{\text{Cy}})_3\text{Fe}^{\text{III}}\text{O}]\text{OTf}$ (**2**), formed during reduction. X-ray photoelectron spectroscopy (XPS) analysis confirms the identity of the Cr^{III} product. These findings build upon the success of complex **1** for oxyanion reduction and offer a promis-



ing pathway for chromium detoxification in environmental applications. More broadly, the development of a paramagnetic ^1H NMR calibration curve establishes a powerful tool for quantitative analysis of a mixture of paramagnetic products.

Author contributions

KLK and CLF carried out the synthetic work. KLK and JMM interpreted the analytical characterizations and contributed to writing and editing the manuscript. ARF provided funding and supervised the studies while aiding in writing and editing the manuscript.

Data availability

The data supporting this article have been included as part of the ESI.†

Conflicts of interest

There are no conflicts to declare.

Acknowledgements

This work was supported by the U.S. Department of Energy, Office of Sciences, Office of Basic Energy Sciences, Chemical Sciences, Geosciences, and Biosciences Division under award number DOE DE-SC002102529. K. L. G. is thankful for a Robert C. & Carolyn J. Springborn Fellowship. J. M. M. is thankful for a Hagler Fellowship.

References

- H. Sun, J. Brocato and M. Costa, *Curr. Environ. Health Rep.*, 2015, **2**, 295.
- B. A. Marinho, R. O. Cristóvão, R. A. R. Boaventura and V. J. P. Vilar, *Environ. Sci. Pollut. Res.*, 2019, **26**, 2203–2227.
- A. Zhitkovich, *Chem. Res. Toxicol.*, 2011, **24**, 1617–1629.
- M. Owlad, M. K. Aroua, W. A. W. Daud and S. Baroutian, *Water, Air, Soil Pollut.*, 2009, **200**, 59–77.
- C. C. Alvarez, M. E. Bravo Gómez and A. Hernández Zavala, *J. Trace Elem. Med. Biol.*, 2021, **65**, 126729.
- M. Ferrari, R. Cozza, M. Marieschi and A. Torelli, *Plants*, 2022, **11**, 223–250.
- Y.-T. Wang, in *Environmental Microbe-Metal Interactions*, ed. D. R. Lovley, Wiley, Hoboken, 2014, **10**, 225–235.
- S. Fendorf, B. W. Wielinga and C. M. Hansel, *Int. Geol. Rev.*, 2000, **42**, 691–701.
- D. Rai, B. M. Sass and D. A. Moore, *Inorg. Chem.*, 1987, **26**, 345–349.
- B. Beverskog and I. Puigdomenech, *Corros. Sci.*, 1997, **39**, 43–57.
- C. M. Stern, T. O. Jegede, V. A. Hulse and N. Elgrishi, *Chem. Soc. Rev.*, 2021, **50**, 1642–1667.
- K. E. Ukhurebor, U. O. Aigbe, R. B. Onyancha, W. Nwankwo, O. A. Osibote, H. K. Paumo, O. M. Ama, C. O. Adetunji and I. U. Siloko, *J. Environ. Manage.*, 2021, **280**, 111809.
- C. M. Stern, D. W. Hayes, L. O. Kgoadi and N. Elgrishi, *Environ. Sci.: Water Res. Technol.*, 2020, **6**, 1256–1261.
- E. M. Matson, Y. J. Park and A. R. Fout, *J. Am. Chem. Soc.*, 2014, **136**, 17398–17401.
- Y. J. Park, M. N. Peñas-Defrutos, M. J. Drummond, Z. Gordon, O. R. Kelly, I. J. Garvey, K. L. Gullett, M. García-Melchor and A. R. Fout, *Inorg. Chem.*, 2022, **61**, 8182–8192.
- C. L. Ford, Y. J. Park, E. M. Matson, Z. Gordon and A. R. Fout, *Science*, 2016, **354**, 741–743.
- M. J. Drummond, T. J. Miller, C. L. Ford and A. R. Fout, *ACS Catal.*, 2020, **10**, 3175–3182.
- K. L. Gullett, C. L. Ford, I. J. Garvey, T. J. Miller, C. A. Leahy, L. N. Awaitey, D. M. Hofmann, T. J. Woods and A. R. Fout, *J. Am. Chem. Soc.*, 2023, **145**, 20868–20873.
- M. M. Abu-Omar, *Comments Inorg. Chem.*, 2003, **24**, 15–37.
- G. Piancatelli, A. Scettri and M. D'Auria, *Synthesis*, 1982, 245–259.
- J. J. Li, *Name Reactions*, Springer, Princeton, 2014.
- G. Cainelli and G. Cardillo, *Chromium Oxidations in Organic Chemistry*, Springer-Verlag, Berlin, 1984.
- J. H. Espenson, *Acc. Chem. Res.*, 1970, **3**, 347–353.
- E. M. Matson, J. A. Bertke and A. R. Fout, *Inorg. Chem.*, 2014, **53**, 4450–4458.
- Y. J. Park, M. N. Peñas-Defrutos, M. J. Drummond, Z. Gordon, O. R. Kelly, I. J. Garvey, K. L. Gullett, M. García-Melchor and A. R. Fout, *Inorg. Chem.*, 2022, **61**, 8182–8192.
- J. M. Moore, T. J. Miller, M. Mu, M. N. Peñas-Defrutos, K. L. Gullett, L. S. Elford, S. Quintero, M. García-Melchor and A. R. Fout, *J. Am. Chem. Soc.*, 2025, **147**, 8444–8454.
- R. S. Drago, *Physical Methods In Chemistry*, Saunders College Publishing, Philadelphia, 1992.
- A. J. Pell, G. Pintacuda and C. P. Grey, *Prog. Nucl. Magn. Reson. Spectrosc.*, 1992, **111**, 1–271.
- L. M. Guard, M. Mohadjer Beromi, G. W. Brudvig, N. Hazari and D. J. Vinyard, *Angew. Chem., Int. Ed.*, 2015, **54**, 13352–13356.
- I. Bertini, C. Luchinat, G. Parigi and E. Ravera, in *Solution NMR of Paramagnetic Molecules*, Elsevier, Amsterdam, 2001, **5**, pp. 175–253.
- C.-C. Wang, X.-D. Du, J. Li, X.-X. Guo, P. Wang and J. Zhang, *Appl. Catal., B*, 2016, **193**, 198–216.
- E. T. Anthony and N. A. Oladoja, *Environ. Sci. Pollut. Res.*, 2022, **29**, 8026–8053.
- M. C. Biesinger, B. P. Payne, A. P. Grosvenor, L. W. M. Lau, A. R. Gerson, R. St and C. Smart, *Appl. Surf. Sci.*, 2011, **257**, 2717–2730.
- M. C. Biesinger, C. Brown, J. R. Mycroft, R. D. Davidson and N. S. McIntyre, *Surf. Interface Anal.*, 2004, **36**, 1550.

